COMMUN. MATH. SCI.
Vol. 13, No. 6, pp. 1639–1648

FAST COMMUNICATION

AN OPTIMIZATION-BASED, HETEROGENEOUS TO HOMOGENEOUS COUPLING METHOD*

ASSYR ABDULLE† AND ORANE JECKER‡

Abstract. An optimization-based algorithm is proposed for solving elliptic problems with highly oscillatory coefficients that do not exhibit scale separation in a subregion of the physical domain. The given method, written as a constrained minimization problem, couples a numerical homogenization method in the subregion of the physical domain with scale separation with a fine scale solver in subregions without scale separation. The unknown boundary conditions of both problems in the overlap region are determined by minimizing the discrepancy of the corresponding solutions in this overlap.

Key words. global-local method, multiscale analysis, homogenization, heterogeneous multiscale method, domain decomposition.

AMS subject classifications. 65N30, 74Q05, 49J20.

1. Introduction

Let $\Omega \subset \mathbb{R}^d$, $d>1$, be a bounded domain, let $f \in L^2(\Omega)$, and consider the following elliptic problem: find $u \in H_0^1(\Omega)$ satisfying

$$-\mathrm{div}\,(a\nabla u) = f, \text{ in } \Omega, \tag{1.1}$$

with $u=0$ on $\partial\Omega$. We assume that the tensor $a \in (L^\infty(\Omega))^{d\times d}$ is symmetric, bounded, highly oscillatory, and uniformly elliptic, that is

$$\alpha|\xi|^2 \le \xi^\top a(x)\xi \le \beta|\xi|^2, \quad \xi \in \mathbb{R}^d, \tag{1.2}$$

with $0<\alpha\le\beta<+\infty$; hence, (1.1) has a unique solution thanks to the Lax–Milgram Theorem.

It is well known that standard numerical methods such as the finite element method (FEM) or the finite volume method (FVM) are inefficient for such problems since convergence can only be obtained if the mesh resolves the smallest scale in the problem which is often computationally prohibitive. To address these issues, there are two broad strategies. The first approach relies on methods using multiscale basis functions obtained by solving the original problem with scale resolution on coarse blocks to obtain a coarse multiscale basis function. The computation of the basis functions, with a cost proportional to the resolution of the finest scale in the problem, requires less storage and can be done in parallel (see [17, 18, 21] and the references therein). The second approach is mainly applied when the coefficients of the problem exhibit scale separation. Then, based on homogenization theory [6, 19], one can build micro-macro methods able to capture the effective solution of (1.1). In this setting, we obtain numerical methods with a computational cost independent of the smallest scale of the problem (see [1, 4, 10] and the references therein). Yet, there are many problems that fall in between

*Received: October 30, 2014; accepted (in revised form): January 20, 2015. Communicated by Weinan E.

†ANMC, Section de Mathématiques, École Polytechnique Fédérale de Lausanne, CH-1015 Lausanne, Switzerland (assyr.abdulle@epfl.ch).

‡ANMC, Section de Mathématiques, École Polytechnique Fédérale de Lausanne, CH-1015 Lausanne, Switzerland (orane.jecker@epfl.ch).

scale and non-scale separations in which scales are separated only in a subdomain of the computational domain. Several multiscale strategies have been proposed to couple a numerical homogenization solver with a fine scale solver in different subdomains. We mention the so called global-local approach, in which the boundary conditions for the fine scale subregions are given by the homogenized solution [22], and the recent L^2 global to local projection method [5].

In this paper, we present a new global local approach combining numerical homogenization methods with ideas coming from the virtual control method developed in [9] and pioneered in [14] and [20]. Our method and analysis are inspired by the recent work for atomistic-to-continuum coupling [23]. Assume that the computational domain Ω is divided into two (overlapping) regions ω and $\omega_2 = \Omega \setminus \omega$ and that the multiscale elliptic problem (1.1) exhibits scale separation in ω_2 but not in ω. Our method couples a multiscale micro-macro method in ω_2 (that approximates an effective problem in that domain) with a fine scale solver in $\omega_1 = \omega \cup \omega_0$, where ω_0 is an overlap region. We notice that the numerical homogenization method on ω_2 involves a finite element method with variational crimes on the macro mesh. To solve the boundary value problems in each subregion, we introduce virtual controls (unknown Dirichlet data in ω_0) that are obtained by minimizing the L^2 norm of the different solutions in the overlap. While the optimization coupling on the overlap minimizes the L^2 norm between the full fine scale solution and the (numerically) homogenized solution in ω_0, we nevertheless get an error estimate with respect to the full fine scale solution in the whole Ω thanks to the use of a Cacciapoli inequality and the reconstruction of the fine scale solution that can be recovered from the known micro and macro solutions in ω_2.

We note that, in the domain decomposition literature, we can find several multiscale coupling techniques for elliptic problems with strong variation in their coefficients as, for example, the domain decomposition method for numerical zooms [16] or the multiscale algorithm with patches of finite elements [13] (see also the references therein). These methods, nevertheless, significantly differ from the method proposed in this paper. Indeed, for these methods to apply, it is assumed that the coefficients of the problems have a multiscale structure only in the zoom or in the patch outside of which they are only slowly varying. Thus, a coarse mesh can be used outside the patch or in the zoom which is not suitable in our case since the multiscale structures are strongly varying in Ω. Hence, these methods and their analysis do not apply in the present context.

In this paper, we introduce our multiscale coupling method and provide an analysis in the continuous case. In a forthcoming paper [3], a full analysis of the numerical method together with numerical comparisons with other coupling strategies will be presented.

2. Optimization-based, heterogeneous to homogeneous coupling

Recall that Ω, a bounded domain, is decomposed as follows: $\Omega = (\Omega \setminus \omega) \cup \omega = \omega_2 \cup \omega$. Consider (1.1) and assume that a can be decomposed into $a = \tilde{a}\chi_\omega + a^\varepsilon(1-\chi_\omega)$, where χ_ω is the indicator function on ω. We further assume that $\omega \Subset \omega_1 \Subset \Omega$ and denote the overlap by $\omega_1 \cap \omega_2 = \omega_0$. Suppose that numerical homogenization holds in ω_2, thus in principle, the solution u can be approximated by $u^0 + \varepsilon u^1$ in ω_2, where u^0 is the solution of (2.2) and u^1 is a corrector term [6, 19]. In contrast, we want to compute a fine scale approximation of u in the domain ω where we do not assume scale separation or stationarity. The above considerations lead to the following coupled problem: denote $\Gamma = \partial\Omega$, $\Gamma_1 = \partial\omega_1$, $\Gamma_2 = \partial\omega$ and consider $u_1 \in H^1(\omega_1)$, $u_2 \in H^1(\omega_2)$ the solutions of

$$-\operatorname{div}(a\nabla u_1) = f, \text{ in } \omega_1, \quad u_1 = \varphi_1, \text{ on } \Gamma_1, \tag{2.1}$$

$$-\mathrm{div}\,(a^0\nabla u_2) = f, \text{ in } \omega_2, \quad u_2 = \varphi_2, \text{ on } \Gamma_2, \quad u_2 = 0 \text{ on } \partial\Omega, \tag{2.2}$$

where the boundary conditions $\varphi_1 \in H^{1/2}(\Gamma_1)$ and $\varphi_2 \in H^{1/2}(\Gamma_2)$ are to be determined. The existence and uniqueness of u_1 and u_2 are given by the Lax–Milgram Theorem provided that φ_1 and φ_2 are known. Let $H^1_\Gamma(\omega_2) := \{u \in H^1(\omega_2) \,|\, u = 0 \text{ on } \Gamma \text{ in the sense of the trace}\}$. The weak formulations read: find $u_1 \in H^1(\omega_1)$ and $u_2 \in H^1_\Gamma(\omega_2)$ solutions of

$$B_i(u_i, v) = \int_{\omega_i} a_i \cdot \nabla u_i \nabla v dx = \int_{\omega_i} f v dx = F_i(v), \quad \forall v \in H^1_0(\omega_i), \text{ for } i = 1,2, \tag{2.3}$$

where $a_1 = a$ and $a_2 = a^0$.

We insist that, for practical calculation, $a^0(x)$ is not available as even in the locally periodic case. Computing this tensor involves yet another boundary value problem; hence, computing $a^0(x)$ amounts to solving infinitely many boundary value problems. Thus, the multiscale method couples

- a finite element approximation $u_{1,\tilde{h}}$ of u_1 in ω_1, where the mesh size $\tilde{h}$ resolves the fine scale in $\tilde{a}(x)$;
- a numerical homogenization finite element approximation $u_{2,H}$ of u_2 in ω_2 recovering the macroscopic data $a^0(x_K)$ using FEM in micro sampling domains around macroscopic quadrature points x_k.

This method, based on the finite element heterogeneous multiscale method (FE-HMM) [1, 2, 10], is detailed in Section 3. Notice that the numerical homogenization method relies on two meshes: a macro triangulation of ω_2 with mesh size H and a micro triangulation of the sampling domains with mesh size h controlling the accuracy of the data $a^0(x_K)$.

Solving problem (2.1)-(2.2) in a constrained optimization setting, as proposed in [11], leads one to consider the artificial boundary conditions φ_i, $i = 1,2$, as control variables and the functions u_i, $i = 1,2$, as state variables. The cost functional to minimize reads

$$J(u_1, u_2) = \frac{1}{2}\|u_1 - u_2\|^2_{L^2(\omega_0)} \tag{2.4}$$

under the constraints that u_1 and u_2 should satisfy (2.1) and (2.2). To solve the above problem, it is convenient to split the solutions u_1 and u_2 into a part depending on the controls and a part solving a homogeneous Dirichlet elliptic problem, as

$$u_1 = u_{1,0} + v_1(\varphi_1) \text{ and } u_2 = u_{2,0} + v_2(\varphi_2),$$

where $u_{1,0}$ and $u_{2,0}$ solve zero Dirichlet boundary value problems in ω_1 and ω_2, respectively. The problem becomes: find $(u_{1,0}, v_1, u_{2,0}, v_2) \in H^1_0(\omega_1) \times H^1(\omega_1) \times H^1_0(\omega_2) \times H^1_\Gamma(\omega_2)$ such that

$$-\mathrm{div}\,(a\nabla u_{1,0}) = f \text{ in } \omega_1, \ u_{1,0} = 0 \quad \text{on } \Gamma_1, \tag{2.5}$$

$$-\mathrm{div}\,(a\nabla v_1) \ = 0 \text{ in } \omega_1, \ v_1 \ = \varphi_1 \text{ on } \Gamma_1, \tag{2.6}$$

and

$$-\mathrm{div}\,(a^0\nabla u_{2,0}) = f \text{ in } \omega_2, \ u_{2,0} = 0 \text{ on } \Gamma, \ u_{2,0} = 0 \quad \text{on } \Gamma_2, \tag{2.7}$$

$$-\mathrm{div}\,(a^0\nabla v_2) \ = 0 \text{ in } \omega_2, \ v_2 \ = 0 \text{ on } \Gamma, \ v_2 \ = \varphi_2 \text{ on } \Gamma_2, \tag{2.8}$$

where we note that the solutions $u_{1,0}$ and $u_{2,0}$ can be computed before performing the coupling since they are independent of the virtual controls. The unknowns become v_1 and v_2.

For a practical implementation, we use the Lagrangian formulation of the above constrained optimization problem, obtained by introducing the Lagrange multipliers $\lambda_1 \in H_0^1(\omega_1)$ and $\lambda_2 \in H_0^1(\omega_2)$ associated to the constraints. The problem then reads: find $(v_1,\lambda_1,v_2,\lambda_2) \in H^1(\omega_1)\times H_0^1(\omega_1)\times H_\Gamma^1(\omega_2)\times H_0^1(\omega_2)$, the critical point of the following Lagrangian functional

$$\mathcal{L}(v_1,\lambda_1,v_2,\lambda_2) = J(u_1,u_2) + \langle f + \operatorname{div}(a\nabla u_1),\lambda_1\rangle_{H^{-1},H^1} + \langle f + \operatorname{div}(a^0\nabla u_2),\lambda_2\rangle_{H^{-1},H^1}. \tag{2.9}$$

Considering next the critical point of (2.9) leads to a saddle point problem

$$\int_{\omega_0}(v_1-v_2)w_1dx - \int_{\omega_1} a\cdot\nabla w_1\nabla\lambda_1 dx = -\int_{\omega_0}(u_{1,0}-u_{2,0})w_1dx,\ \forall w_1\in H^1(\omega_1), \tag{L1}$$

$$\int_{\omega_1} a\cdot\nabla v_1\nabla\xi_1 dx = \int_{\omega_1} f\xi_1 dx - \int_{\omega_1} a\cdot\nabla u_{1,0}\nabla\xi_1 dx, \qquad \forall\xi_1\in H_0^1(\omega_1), \tag{L2}$$

$$-\int_{\omega_0}(v_1-v_2)w_2dx - \int_{\omega_2} a^0\cdot\nabla w_2\nabla\lambda_2 dx = \int_{\omega_0}(u_{1,0}-u_{2,0})w_2dx, \forall w_2\in H_\Gamma^1(\omega_2), \tag{L3}$$

$$\int_{\omega_2} a^0\cdot\nabla v_2\nabla\xi_2 dx = \int_{\omega_2} f\xi_2 dx - \int_{\omega_2} a^0\cdot\nabla u_{2,0}\nabla\xi_2 dx, \qquad \forall\xi_2\in H_0^1(\omega_2). \tag{L4}$$

We note that the well-posedness of the optimization-based problem can be established from (L1)–(L4) using Brezzi's theory [7].

3. Multiscale coupling method

The method couples the FEM in ω_1 with the FE-HMM in ω_2, hence the mesh H in ω_2 can be larger than ε and the mesh size $\tilde{h}$ in ω_1 should be smaller than the fine scales; an example is illustrated in Figure 3.1.

Let $\mathcal{T}_{\tilde{h}}$ be a triangulation of ω_1 with mesh size given by $\tilde{h} = \max_{K\in\mathcal{T}_{\tilde{h}}} h_K$. In addition, we suppose that the triangulation is admissible and shape regular in the sense of [8].

We define a FE space of degree p over $\mathcal{T}_{\tilde{h}}$ by

$$V^p(\omega_1,\mathcal{T}_{\tilde{h}}) = \{w\in H^1(\omega_1)\,|\,w|_K\in\mathcal{R}^p(K),\forall K\in\mathcal{T}_{\tilde{h}}\},$$

where $\mathcal{R}^p(K)$ is the space $\mathcal{P}^p(K)$ of polynomials on K of degree at most p if the element K is simplicial, or the space $\mathcal{Q}^p(K)$ of polynomials on K of degree at most p in each variable if K is a rectangular FE. We use $V_0^p(\omega_1,\mathcal{T}_{\tilde{h}})$ to denote the elements of $V^p(\omega_1,\mathcal{T}_{\tilde{h}})$ that vanish on $\partial\omega_1$. For the FE-HMM in ω_2, we need macro and micro partitions. Let $\mathcal{T}_H$ be a triangulation of ω_2 with mesh size $H = \max_{K\in\mathcal{T}_H} h_K$ that can be larger than ε. We suppose that $\mathcal{T}_H$ is also admissible and regular.

Macro Finite Element space. The macro FE space over $\mathcal{T}_H$ is defined by

$$V_\Gamma^p(\omega_2,\mathcal{T}_H) = \{w\in H_\Gamma^1(\omega_2)\,|\,w|_K\in\mathcal{R}^p(K),\forall K\in\mathcal{T}_H\}.$$

We use $V_0^p(\omega_2,\mathcal{T}_H)$ to denote the FE space of degree p of functions that vanish on $\partial\omega_2$. Within each element $K\in\mathcal{T}_H$, we consider integration points $x_{j,K}\in K$ with quadrature weight $w_{j,K}$ for $j=1,\dots,J$ and around each integration point we construct a sampling domain $K_{\delta_j} = x_{j,K} + \delta I$, where $I = (-1/2,1/2)$.

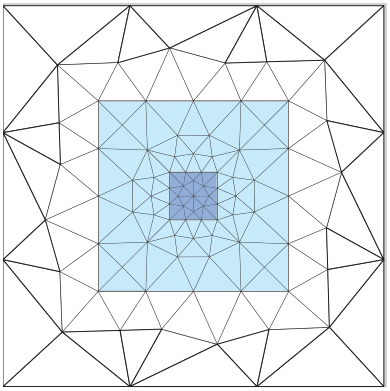

FIG. 3.1. *Illustration of a mesh over a domain* $\Omega=[0,1]^2$ *with* ω_0 *in light blue and* ω *in dark blue.*

Quadrature formula (QF). We denote by $\hat{K}$ the reference macro element, and, for all $K\in\mathcal{T}_H\cup\mathcal{T}_{\tilde{h}}$, we consider a mapping F_K such that $F_K(\hat{K})=K$. Suppose that we have a QF on $\hat{K}$ with quadrature points and weights $\{\hat{x}_j,\hat{w}_j\}_{j=1}^J$. A QF on K is given via $x_{j,K}=F_K(\hat{x_j})$ and $w_{j,K}=\hat{w}_j\det(\partial F_K)$, for $j=1,\dots,J$. We state the usual assumption for a QF when using a FEM with numerical integration (see [8, Chapter 4.1]):

(Q1) $\hat{w}_j>0$, $j=1,\dots,J$ and $\sum_{j=1}^J\hat{w}_j|\nabla\hat{p}(\hat{x}_j)|^2\geq\hat{\lambda}\|\nabla\hat{p}\|^2_{\mathrm{L}^2(\hat{K})}$, $\forall\hat{p}(\hat{x})\in\mathcal{R}^p(\hat{K})$;

(Q2) $\int_{\hat{K}}\hat{p}(\hat{x})d\hat{x}=\sum_{j=1}^J\hat{w}_j\hat{p}(\hat{x}_j),\forall\hat{p}(\hat{x})\in\mathcal{R}^\sigma(\hat{K})$, for $\sigma=\max\{2p-2,p\}$ if $\hat{K}$ is simplicial and $\sigma=\max\{2p-1,p+1\}$ if $\hat{K}$ is rectangular.

Micro Finite Element space. On each of the sampling domains K_{δ_j}, we consider a micro partition $\mathcal{T}_h$ of elements Q with diameter h_Q, and we denote $h=\max_{Q\in\mathcal{T}_h}h_Q$, $h<\varepsilon$. The FE space of degree q is given by

$$S^q(K_{\delta_j},\mathcal{T}_h)=\{w\in W(K_{\delta_j})\,|\,w|_Q\in\mathcal{R}^q(Q),Q\in\mathcal{T}_h\},$$

where the Sobolev space $W(K_{\delta_j})$ determines the type of coupling between the macro and micro problems ($W(K_{\delta_j})=W^1_{\mathrm{per}}(K_{\delta_j})$ for periodic or $W(K_{\delta_j})=H^1_0(K_{\delta_j})$ for Dirichlet).11

With the definition of the FE spaces, we state the discretization of Equation (2.3) for u_1. It reads: find $u_{1,\tilde{h}}\in V^p(\omega_1,\mathcal{T}_{\tilde{h}})$, a solution of

$$B_1(u_{1,\tilde{h}},w_{\tilde{h}})=\int_{\omega_1}a\cdot\nabla u_{1,\tilde{h}}\nabla w_{\tilde{h}}dx=\int_{\omega_1}fw_{\tilde{h}}dx=F_1(w_{\tilde{h}}),\quad\forall w_{\tilde{h}}\in V_0^p(\omega_1,\mathcal{T}_{\tilde{h}}).\tag{3.1}$$

For the discretization of (2.3) for u_2, we construct a macro bilinear form for $u_{2,H},w_{2,H}\in V^p_\Gamma(\omega_2,\mathcal{T}_H)$,

$$B_{2,H}(u_H,w_H)=\sum_{K\in\mathcal{T}_H}\sum_{j=1}^J\frac{w_{j,K}}{|K_{\delta_j}|}\int_{K_{\delta_j}}a^\varepsilon\cdot\nabla u_j^h\nabla w_j^h dx,$$

where u_j^h,w_j^h are micro functions defined on K_{δ_j} in the following way: find u_j^h such that

$u_j^h - u_{2,H,\mathrm{lin},j} \in S^q(K_{\delta_j}, \mathcal{T}_h)$ and

$$\int_{K_{\delta_j}} a^\varepsilon \cdot \nabla v_j^h \nabla w dx = 0, \quad \forall w \in S^q(K_{\delta_j}, \mathcal{T}_h),$$

where $u_{2,H,\mathrm{lin},j}(x) = u_{2,H}(x_{j,K}) + (x - x_{j,K}) \cdot \nabla u_{2,H}(x_{j,K})$. Then, the discretization of (2.3) for u_2 reads: find $u_{2,H} \in V_\Gamma^p(\omega_2, \mathcal{T}_H)$, a solution of

$$B_{2,H}(u_{2,H}, w_{2,H}) = F_2(w_{2,H}), \quad \forall w_{2,H} \in V_0^p(\omega_2, \mathcal{T}_H). \tag{3.2}$$

The discrete system for the optimization based coupling problem is: find $(v_{1,\tilde{h}}, \lambda_{1,\tilde{h}}, v_{2,H}, \lambda_{2,H}) \in V^p(\omega_1, \mathcal{T}_{\tilde{h}}) \times V_0^p(\omega_1, \mathcal{T}_{\tilde{h}}) \times V_\Gamma^p(\omega_2, \mathcal{T}_H) \times V_0^p(\omega_2, \mathcal{T}_H)$, a solution of

$$\int_{\omega_0} (v_{1,\tilde{h}} - v_{2,H}) w_{1,\tilde{h}} dx - B_1(w_{1,\tilde{h}}, \lambda_{1,\tilde{h}}) = -\int_{\omega_0} (u_{1,0,\tilde{h}} - u_{2,0,H}) w_{1,\tilde{h}} dx, \tag{L1b}$$

$$B_1(v_{1,\tilde{h}}, \xi_{1,\tilde{h}}) = F_1(\xi_{1,\tilde{h}}) - B_1(u_{1,0,\tilde{h}}, \xi_{1,\tilde{h}}), \tag{L2b}$$

$$-\int_{\omega_0} (v_{1,\tilde{h}} - v_{2,H}) w_{2,H} dx - B_{2,H}(w_{2,H}, \lambda_{2,H}) = \int_{\omega_0} (u_{1,0,\tilde{h}} - u_{2,0,H}) w_{2,H} dx, \tag{L3b}$$

$$B_{2,H}(v_{2,H}, \xi_{2,H}) = F_2(\xi_{2,H}) - B_{2,H}(u_{2,0,H}, \xi_{2,H}), \tag{L4b}$$

for all $w_{1,\tilde{h}} \in V^p(\omega_1, \mathcal{T}_{\tilde{h}})$, $\xi_{1,\tilde{h}} \in V_0^p(\omega_1, \mathcal{T}_{\tilde{h}})$, $w_{2,H} \in V_\Gamma^p(\omega_2, \mathcal{T}_H)$, and $\xi_{2,H} \in V_0^p(\omega_2, \mathcal{T}_H)$.

Then, using a FE basis for $\mathcal{T}_{\tilde{h}}$ and $\mathcal{T}_H$, we are able to write the system (L1b)-(L4b) in a matrix form:

$$\begin{pmatrix} M & B^\top \\ B & 0 \end{pmatrix} U = G,$$

where $U = (v_{1,\tilde{h}}, v_{2,H}, \lambda_{1,\tilde{h}}, \lambda_{2,H})^\top$. This system can be solved without an optimization iteration since it is possible to solve the system using computational methods (this approach is called the one-shot method [15]).

The algorithm is as follows:

1. Compute $u_{1,0,\tilde{h}} \in V_0^p(\omega_1, \mathcal{T}_{\tilde{h}})$ with (3.1) using FEM over $\mathcal{T}_{\tilde{h}}$.
2. Compute $u_{2,0,H} \in V_0^p(\omega_2, \mathcal{T}_H)$ with (3.2) using FE-HMM over $\mathcal{T}_H$.
3. Compute $v_{1,\tilde{h}} \in V^p(\omega_1, \mathcal{T}_{\tilde{h}})$ and $v_{2,H} \in V_\Gamma^p(\omega_2, \mathcal{T}_H)$ by solving the system (L1b)-(L4b).

4. A priori error analysis

In this section, we discuss the accuracy of our coupling method. We emphasize that we do not address the fully discrete analysis; that is postponed to a forthcoming publication [3]. Let $\bar{u}$ denote the solution of the optimization-based coupling given by

$$\bar{u} = \begin{cases} u_{1,0} + v_1(\varphi_1) \text{ in } \omega_1, \\ u_{2,0} + v_2(\varphi_2) \text{ in } \omega_2 \setminus \omega_0, \end{cases} \tag{4.1}$$

where $u_{1,0}$, v_1, $u_{2,0}$, and v_2 are solutions of (2.5), (2.6), (2.7), and (2.8) respectively. We give an analysis for the error $\|\nabla(u - \bar{u})\|_{\mathrm{L}^2(\omega)}$, where u is the solution of (1.1).

We first establish the well-posedness of the optimization problem (2.4) and consider $J(u_1, u_2) = \tilde{J}(\varphi_1, \varphi_2)$ defined as

$$\tilde{J}(\varphi_1, \varphi_2) = \frac{1}{2} \|v_1(\varphi_1) - v_2(\varphi_2)\|_{L^2(\omega_0)}^2 + \frac{1}{2} \|u_{1,0} - u_{2,0}\|_{L^2(\omega_0)}^2$$

$$+\int_{\omega_0}(u_{1,0}-u_{2,0})(v_1(\varphi_1)-v_2(\varphi_2))dx.$$

Let $\mathcal{U}:=H^{1/2}(\Gamma_1)\times H^{1/2}(\Gamma_2)$. The constrained optimization problem then reads: find $(\varphi_1,\varphi_2)\in\mathcal{U}$ such that $\tilde{J}(\varphi_1,\varphi_2)=\frac{1}{2}\|u_1(\varphi_1)-u_2(\varphi_2)\|_{L^2(\omega_0)}$ is minimized subject to equations (2.1) and (2.2). The necessary optimality condition is obtained by the Euler–Lagrange equation: find $(\varphi_1,\varphi_2)\in\mathcal{U}$ such that

$$\pi(\{\varphi_1,\varphi_2\},\{\mu_1,\mu_2\})=-\int_{\omega_0}(u_{1,0}-u_{2,0})(v_1(\mu_1)-v_2(\mu_2))dx,\quad\forall(\mu_1,\mu_2)\in\mathcal{U},\tag{4.2}$$

where the bilinear form π is given by
$\pi(\{\varphi_1,\varphi_2\},\{\mu_1,\mu_2\})=\int_{\omega_0}(v_1(\varphi_1)-v_2(\varphi_2))(v_1(\mu_1)-v_2(\mu_2))dx$. Following standard arguments, it can be shown that π defines an inner product on the space $\mathcal{U}$, and the existence and uniqueness of a minimizer in the space $\hat{\mathcal{U}}$, obtained by completion for the norm $\|\cdot\|_{L^*(\mathcal{U})}$ induced by π, is obtained using the Riesz-Representation Theorem (see [11] for details).

We next establish an a priori error estimate for the coupling error by estimating $u-\bar{u}$. Since $u-\bar{u}$ is a-harmonic in ω_1, the Caccioppoli inequality [12] can be used to bound the H^1 seminorm on ω by the L^2 norm on ω_1. Let τ denote the width of ω_0 and recall that $0<\alpha\le\beta<+\infty$ are the coercivity constants of a given by (1.2); we then have

$$\|\nabla(u-\bar{u})\|_{\mathrm{L}^2(\omega)}\le C(\tau,\beta,\alpha)\|u-\bar{u}\|_{\mathrm{L}^2(\omega_1)}.$$

For any couple of controls $\{\mu_1,\mu_2\}\in\mathcal{U}$, we define an operator $P:\mathcal{U}\to H^1_0(\Omega)$ by

$$\{\mu_1,\mu_2\}\mapsto P(\{\mu_1,\mu_2\})=\begin{cases}u_{1,0}+v_1(\mu_1)\text{ in }\omega_1,\\ u_{2,0}+v_2(\mu_2)\text{ in }\omega_2\setminus\omega_0,\end{cases}$$

which can be split into $P=U_0+Q$ where U_0 is the constant part of P and

$$Q(\{\mu_1,\mu_2\})=\begin{cases}v_1(\mu_1)\text{ in }\omega_1,\\ v_2(\mu_2)\text{ in }\omega_2\setminus\omega_0.\end{cases}$$

Moreover, we define the trace operator $\gamma:H^1_0(\Omega)\to\mathcal{U}$ by $\gamma(u)=(\gamma_1(u),\gamma_2(u))$, where $\gamma_i:H^1(\omega_i)\to H^{1/2}(\Gamma_i)$, $i=1,2$, is given by $\gamma_i(u)=u|_{\Gamma_i}$ (in the sense of the trace). Using the exact trace of u as boundary condition in problem (2.8), we define

$$u^c=u_{2,0}+v_2(\gamma_2(u))$$

and observe that $u|_{\omega_1}=(u_{1,0}+v_1(\gamma_1(u)))|_{\omega_1}$. Then, we have

$$\begin{aligned}\|u-\bar{u}\|_{L^2(\omega_1)}&=\|u-P(\{\varphi_1,\varphi_2\})\|_{L^2(\omega_1)}\\&\le\underbrace{\|u-P(\gamma(u))\|_{L^2(\omega_1)}}_{=0}+\|P(\gamma(u))-P(\{\varphi_1,\varphi_2\})\|_{L^2(\omega_1)}\\&\le\|Q\|\|\gamma(u)-\{\varphi_1,\varphi_2\}\|_{L^*(\mathcal{U})},\end{aligned}\tag{4.3}$$

where the norm of the operator Q is

$$\|Q\|=\sup_{\{\mu_1,\mu_2\}}\frac{\|Q(\{\mu_1,\mu_2\})\|_{L^2(\Omega)}}{\|\{\mu_1,\mu_2\}\|_{L^*(\mathcal{U})}}.$$

A bound on the norm $\|\gamma(u)-\{\varphi_1,\varphi_2\}\|$ is given in the next lemma, assuming local periodic coefficients a in ω_2. For the proof we refer to [3].

LEMMA 4.1. *Let u be the solution of* (1.1) *and let $\{\varphi_1,\varphi_2\}$ be the minimizer of* (4.2). *Then,*

$$\|\gamma(u)-\{\varphi_1,\varphi_2\}\|_{L^*(\mathcal{U})}\leq\|u-u^c\|_{L^2(\omega_0)}$$

Moreover, it holds that $\|u-u^c\|_{L^2(\omega_0)}\leq C\varepsilon.$

Finally, we obtain the following error bound.

THEOREM 4.2. *Let u, $\bar{u}$ be solutions of* (1.1) *and* (4.1) *respectively. We have*

$$\|\nabla(u-\bar{u})\|_{\mathrm{L}^2(\omega)}\leq C\varepsilon, \tag{4.4}$$

where the constant C depends on Q, τ, α, β, and on the domains ω_1 and ω_2.

The last step for the error analysis is to bound the norm of the operator Q in (4.4) that depends on the size of the overlapping domain and the size of the subdomains. This will be discussed in [3] as well as an error estimate for the FEM - FE-HMM discretization described in Section 3.

5. Numerical experiments

In this section, we present numerical experiments on two examples for our new coupling method. Comparisons with other methods will be presented in a forthcoming paper. In the two examples, we take a highly heterogeneous non-periodic tensor with oscillations at several non-separated scales in ω, denoted by $\tilde{a}(x_1,x_2)$, and a locally periodic tensor in $\Omega\setminus\omega$ (with period ε), denoted by $a^\varepsilon(x_1,x_2)$ (see also Figures 5.1(a) and 5.1(d)). We then

1. fix ε and compute the H^1 norm of the exact solution for different widths τ of the overlap using a refinement of the fine scale mesh,
2. take different values of ε and see the influence of the locally periodic wavelength in the coupling strategy.

For simplicity, we suppose that the mesh is continuous in Ω and that $\mathcal{T}_H$ and $\mathcal{T}_{\tilde{h}}$ are identical in ω_0. We use P_1-FE and compute an approximation of u using FEM on a very fine mesh over Ω. Figures 5.1(b)-5.1(e) indicate the convergence of the coupling algorithm (for the numerical solution) with successive smaller mesh sizes in ω (with various sizes of overlap) while Figures 5.1(c)-5.1(f) illustrate the convergence of the optimization-based solution stated in Theorem 4.2 for the numerical solution.

Example 1. Let $a(x_1,x_2)=\tilde{a}(x_1,x_2)\chi_\omega(x_1,x_2)+a^\varepsilon(x_1,x_2)(1-\chi_\omega(x_1,x_2))$ where

$$\tilde{a}(x_1,x_2)=\ 3+\frac{1}{7}\sum_{j=0}^{4}\sum_{i=0}^{j}\frac{2}{j+1}\cos\left(\left\lfloor 8\left(ix_2-\frac{x_1}{i+1}\right)\right\rfloor+\lfloor 150ix_1\rfloor+\lfloor 150x_2\rfloor\right),$$

$$a^\varepsilon(x_1,x_2)=\frac{1}{6}\left(\frac{1.1+\sin(2\pi(x_1/\varepsilon)(x_2/\varepsilon))}{1.1+\sin(2\pi x_2/\varepsilon)}+\sin(4x_1^2x_2^2)+2\right)I.$$

1. Let $\varepsilon=1/160$. The convergence rate $\|u-u_{\tilde{h}H}\|_{\mathrm{H}^1(\omega)}$ is given in Figure 5.1(b) for $\tau=\frac{3}{16}$ (full), $\tau=\frac{1}{16}$ (dashed), and $\tau=\frac{3}{80}$ (dotted lines).
2. For an initial DOF of $N_\varepsilon=7$ points per ε, the error $\|u-u_{\tilde{h}H}\|_{\mathrm{H}^1(\omega)}$ is given in Figure 5.1(c) for $\varepsilon=\frac{1}{4}$ (full), $\varepsilon=\frac{1}{8}$ (dashed), and $\varepsilon=\frac{1}{12}$ (dotted lines).

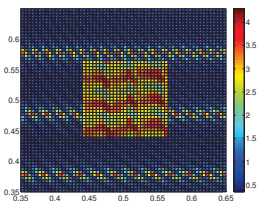

(a) *Example 1: tensor a for* $\varepsilon = 1/10$.

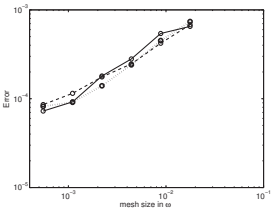

(b) *Example 1:* H^1 *norm for* $\tau = 3/16$*(full),* $\tau = 1/8$ *(dashed), and* $\tau = 1/16$ *(dotted), for* $\varepsilon = 1/160$.

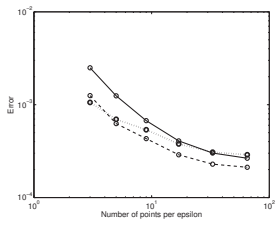

(c) *Example 1:* H^1 *norm for* $\varepsilon = 1/4$*(full),* $\varepsilon = 1/8$ *(dashed), and* $\varepsilon = 1/12$ *(dotted), for* $\tau = 3/16$.

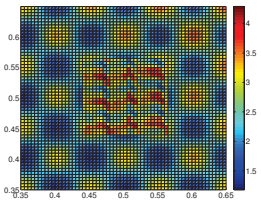

(d) *Example 2: tensor a for* $\varepsilon = 1/10$.

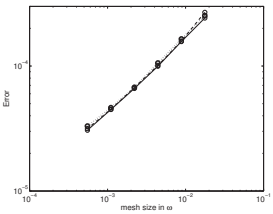

(e) *Example 2:* H^1 *norm for* $\tau = 3/16$*(full),* $\tau = 1/8$ *(dashed), and* $\tau = 1/16$ *(dotted), for* $\varepsilon = 1/160$.

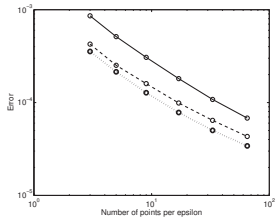

(f) *Example 2:* H^1 *norm for* $\varepsilon = 1/4$*(full),* $\varepsilon = 1/8$ *(dashed), and* $\varepsilon = 1/12$ *(dotted), for* $\tau = 3/16$.

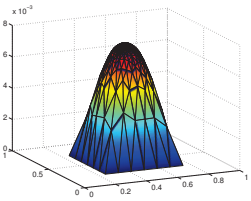

(g) *Example 2: numerical solution* $u_{1,0}$ *for* $\varepsilon = 1/160$ *and* $\tau = 3/16$.

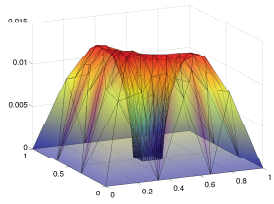

(h) *Example 2: numerical solution* $u_{2,0}$ *for* $\varepsilon = 1/160$ *and* $\tau = 3/16$.

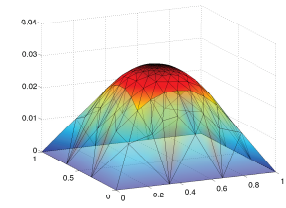

(i) *Example 2: numerical solutions* u_1 *(full) and* u_2 *(transparent) for* $\varepsilon = 1/160$ *and* $\tau = 3/16$.

FIG. 5.1.

Example 2. Let $a(x_1,x_2) = \tilde{a}(x_1,x_2)\chi_\omega(x_1,x_2) + a^\varepsilon(x_1,x_2)(1-\chi_\omega(x_1,x_2))$ be given by

$$\tilde{a}(x_1,x_2) = 3 + \frac{1}{7}\sum_{j=0}^{4}\sum_{i=0}^{j}\frac{2}{j+1}\cos\left(\left\lfloor 8\left(ix_2 - \frac{x_1}{i+1}\right)\right\rfloor + \lfloor 150ix_1\rfloor + \lfloor 150x_2\rfloor\right),$$

$$a^\varepsilon(x_1,x_2) = \left(2.1 + \cos(2\pi x_1/\varepsilon)\cos(2\pi x_2/\varepsilon) + \sin(4x_1^2x_2^2)\right)I.$$

1. Let $\varepsilon = 1/160$. The convergence rate $\|u - u_{\tilde{h}H}\|_{\mathrm{H}^1(\omega)}$ is given in Figure 5.1(e) for $\tau = \frac{3}{16}$ (full), $\tau = \frac{1}{16}$ (dashed), and $\tau = \frac{3}{80}$ (dotted lines). Numerical solutions $u_{1,0}, u_{2,0}$, and $\bar{u}$ are shown in Figures 5.1(g), 5.1(h), and 5.1(i) respectively.
2. For an initial DOF of $N_\varepsilon = 7$ points per ε, the error $\|u - u_{\tilde{h}H}\|_{\mathrm{H}^1(\omega)}$ is given in Figure 5.1(f) for $\varepsilon = \frac{1}{4}$ (full), $\varepsilon = \frac{1}{8}$ (dashed), and $\varepsilon = \frac{1}{12}$ (dotted lines).

Acknowledgement. This work is partially supported by the Swiss National Foundation.

REFERENCES

[1] A. Abdulle, *The finite element heterogeneous multiscale method: a computational strategy for multiscale PDEs*, in Multiple Scales Problems in Biomathematics, Mechanics, physics and numerics, GAKUTO Internat. Ser. Math. Sci. Appl., Gakkōtosho, Tokyo, 31, 133–181, 2009.

[2] A. Abdulle, *A priori and a posteriori error analysis for numerical homogenization: A unified framework*, Ser. Contemp. Appl. Math. CAM, 16, 280–305, 2011.

[3] A. Abdulle, O. Jecker, and A.V. Shapeev, *A priori error analysis of fully discrete optimization based coupling method for multiscale problems*, in preparation.

[4] I. Babuška, *Homogenization and its application. Mathematical and computational problems*, in Numerical solution of partial differential equations, III (Proc. Third Sympos. (SYNSPADE), Univ. Maryland, College Park, Md., 1975), Academic Press, New York, 89–116, 1976.

[5] I. Babuška and R. Lipton, *L2-global to local projection an approach to multiscale analysis*, Math. Model. Meth. Appl. Sci., 21, 2211–2226, 2011.

[6] A. Bensoussan, J.-L. Lions, and G. Papanicolaou, *Asymptotic Analysis for Periodic Structures*, North-Holland Publishing Co., Amsterdam, 1978.

[7] F. Brezzi, *On the existence, uniqueness and approximation of saddle-point problems arising from Lagrangian multipliers*, ESAIM Math. Model. Numer. Anal., 8(R2), 129–151, 1974.

[8] P.G. Ciarlet, *The Finite Element Method for Elliptic Problems*, Stud. Math. Appl., North-Holland, 4, 1978.

[9] M. Discacciati, P. Gervasio, and A. Quarteroni, *The interface control domain decomposition (icdd) method for elliptic problems*, SIAM J. Control Optim., 51(5), 3434–3458, 2013.

[10] W. E and B. Engquist, *The heterogeneous multiscale methods*, Commun. Math. Sci., 1(1), 87–132, 2003.

[11] P. Gervasio, J.-L. Lions, and A. Quarteroni, *Heterogeneous coupling by virtual control methods*, Numer. Math., 90, 241–264, 2000.

[12] M. Giaquinta, *Multiple Integrals in the Calculus of Variations and Nonlinear Elliptic Systems*, Princeton University Press, 1983.

[13] R. Glowinski, J. He, J. Rappaz, and J. Wagner, *A multi-domain method for solving numerically multi-scale elliptic problems*, C.R. Math. Acad. Sci. Paris, 338(9), 741–746, 2004.

[14] R. Glowinski, J. Périaux, and G. Terrasson, *On the coupling of viscous and inviscid models for compressible fluid flows via domain decomposition*, Domain Decomposition Meth. Part. Diff. Eqs., 64–97, 1990.

[15] M.D. Gunzburger, *Perspectives in Flow Control and Optimization*, SIAM, 2003.

[16] F. Hecht, A. Lozinski, and O. Pironneau, *Numerical zoom and the Schwarz algorithm*, in Domain Decomposition Methods in Science and Engineering XVIII, Lect. Notes Comput. Sci. Eng., Springer, Berlin, 70, 63–73, 2009.

[17] T.Y. Hou and X.H. Wu, *A multiscale finite element method for elliptic problems in composite materials and porous media*, J. Comput. Phys., 134(1), 169–189, 1997.

[18] T.J.R. Hughes, G.R. Feijóo, L. Mazzei, and J.B. Quincy, *The variational multiscale method—a paradigm for computational mechanics*, Comput. Meth. Appl. Mech. Engrg., 166(1-2), 3–24, 1998.

[19] V.V. Jikov, S.M. Kozlov, and O.A. Oleinik, *Homogenization of Differential Operators and Integral Functionals*, Springer-Verlag, Berlin, Heidelberg, 1994.

[20] J.L. Lions and O. Pironneau, *Sur le contrôle parallèle des systèmes distribués*, C.R. Acad. Sci., 993–998, 1998.

[21] A. Målqvist and D. Peterseim, *Localization of elliptic multiscale problems*, Math. Comput., 83(290), 2583–2603, 2014.

[22] J.T. Oden and K.S. Vemaganti, *Estimation of local modeling error and goal-oriented adaptive modeling of heterogeneous materials. I. Error estimates and adaptive algorithms*, J. Comput. Phys., 164(1), 22–47, 2000.

[23] D. Olson, P.B. Bochev, M. Luskin, and A.V. Shapeev, *An optimization-based atomistic-to-continuum coupling method*, SIAM J. Numer. Anal., 52(4), 2183–2204, 2014.